Inorg. Chem. **2008**, *47*, 5162−5168

Inorganic Chemistry
Article

Syntheses, Structures, Photoluminescence, and Magnetic Properties of Phenanthrene-Based Carboxylic Acid Coordination Polymers

Zhaorui Pan,[†] You Song,[†] Yan Jiao,[‡] Zhijie Fang,[‡] Yizhi Li,[†] and Hegen Zheng*[,†,§]

State Key Laboratory of Coordination Chemistry, School of Chemistry and Chemical Engineering, Laboratory of Solid State Microstructures, Nanjing University, Nanjing 210093, P. R. China, School of Chemical Engineering, Nanjing University of Science & Technology, Nanjing, 210094, P. R. China, and State Key Laboratory of Structural Chemistry, Fujian Institute of Research on the Structure of Matter, Chinese Academy of Sciences, Fuzhou 350002, P. R. China

Received December 21, 2007

Four new coordination complexes, $M_2(Htmopa)_4(H_2O)_4$ (M = Zn^{2+} (**1**), Mn^{2+} (**2**), $\{M(Htmopa)_2(H_2O)_2\}_n$ (M = Ni^{2+} (**3**), Co^{2+} (**4**)), have been synthesized by the hydrothermal reaction of Htmopa (Htmopa = 2,3,6,7-tetramethoxyphenanthrene-9-carboxylic acid) with different transition metals at a suitable temperature. Single-crystal determinations revealed that **1** and **2** are isostructural and possess a dinuclear subunit, each connected into 3D networks by hydrogen bonds and C−H$\cdots\pi$ interactions. **3** and **4** are also isostructural: the metal ions are bridged through water molecules and carboxylate oxygen atoms to form 1D wavelike double chains, and these double chains are further extended to a 3D network via hydrogen bonds and C−H$\cdots\pi$ interactions. The photoluminescent properties of the free Htmopa ligand and its complexes have been studied in the solid state at room temperature. Both Htmopa and **1** exhibit strong blue emissions. Magnetic susceptibility measurements indicate that **2** and **3** exhibit antiferromagnetic coupling, whereas **4** shows a ferromagnetic coupling and exhibits a single-ion behavior of the Co^{II} ion at a higher temperature range.

Introduction

Transition-metal coordination compounds have recently attracted increasing attention because of their novel architectures[1–4] and useful physical properties such as magnetism,[5–7] photoluminescence,[8,9] nonlinear optical properties,[10] and catalysis.[11] The design of molecular magnetic materials, such as single molecule magnets and single chain magnets, has been extensively explored in recent years.[12–16] Bridging ligands can efficiently propagate magnetic superexchange between metal centers, so the basic strategy to design such

---

* To whom correspondence should be addressed. E-mail: zhenghg@nju.edu.cn. Fax: 86-25-83314502.

[†] Nanjing University.

[‡] Nanjing University of Science & Technology.

[§] Fujian Institute of Research on the Structure of Matter, Chinese Academy of Sciences.

(1) (a) Li, H.; Eddaoudi, M.; O'Keeffe, M.; Yaghi, O. M. *Nature.* **1999**, *402*, 276–279. (b) Yaghi, O. M.; Li, H. L.; Davis, C.; Richardson, D.; Groy, T. L. *Acc. Chem. Res.* **1998**, *31*, 474–484. (c) Walton, K. S.; Snurr, R. Q. *J. Am. Chem. Soc.* **2007**, *129*, 8552–8556.

(2) (a) Kondo, M.; Yoshitomi, T.; Seki, K.; Matsuzaka, H.; Kitagawa, S. *Angew. Chem., Int. Ed.* **1997**, *36*, 1725–1727. (b) Noro, S. I.; Kitagawa, S.; Kondo, M.; Seki, K. *Angew. Chem., Int. Ed.* **2000**, *39*, 2081–2084.

(3) (a) Chen, B.; Eddaoudi, M.; Reineke, T. M.; Kampf, J. W.; O'Keeffe, M.; Yaghi, O. M. *J. Am. Chem. Soc.* **2000**, *122*, 11559–11561. (b) Eddaoudi, M.; Li, H. L.; Yaghi, O. M. *J. Am. Chem. Soc.* **2000**, *122*, 1391–1397.

(4) Seo, J. S.; Whang, D.; Lee, H.; Jun, S. I.; Oh, J.; Jeon, Y. J.; Kim, K. *Nature* **2000**, *404*, 982–986.

(5) (a) Sessoli, R.; Gatteschi, D.; Caneschi, A.; Novak, M. A. *Nature* **1993**, *365*, 141–143. (b) Wernsdorfer, W.; Aliaga-Alcalde, N.; Hendrickson, D. N.; Christou, G. *Nature* **2002**, *416*, 406–409. (c) Sessoli, R.; Tsai, H. L.; Schake, A. R.; Wang, S.; Vincent, J. B.; Folting, K.; Gatteschi, D.; Christou, G.; Hendrickson, D. N. *J. Am. Chem. Soc.* **1993**, *115*, 1804–1816. (d) Ruiz, D.; Sun, Z.; Albela, B.; Folting, K.; Christou, G.; Hendrickson, D. N. *Angew. Chem., Int. Ed.* **1998**, *37*, 300–302. (e) Gatteschi, D.; Sessoli, R. *Angew. Chem., Int. Ed.* **2003**, *42*, 268–297. (f) Oshio, H.; Hoshino, N.; Ito, T.; Nakano, M. *J. Am. Chem. Soc.* **2004**, *126*, 8805–8812. (g) Stamatatos, T. C.; Foguet-Albiol, D.; Stoumpos, C. C.; Raptopoulou, C. P.; Terzis, A.; Wernsdorfer, W.; Perlepes, S. P.; Christou, G. *J. Am. Chem. Soc.* **2005**, *127*, 15380–15381. (h) Ni, Z.-H.; Kou, H. Z.; Zhang, L. F.; Ge, C.; Cui, A. L.; Wang, R. J.; Li, Y. D.; Sato, O. *Angew. Chem., Int. Ed.* **2005**, *44*, 7742–7745.

(6) (a) Caneschi, A.; Gatteschi, D.; Lalioti, N.; Sangregorio, C.; Sessoli, R.; Venturi, G.; Vindigni, A.; Rettori, A.; Pini, M. G.; Novak, M. A. *Angew. Chem., Int. Ed.* **2001**, *40*, 1760–1763. (b) Clérac, R.; Miyasaka, H.; Yamashita, M.; Coulon, C. J. *J. Am. Chem. Soc.* **2002**, *124*, 12837–12844. (c) Liu, T. F.; Fu, D.; Gao, S.; Zhang, Y. Z.; Sun, H. L.; Su, G.; Liu, Y. J. *J. Am. Chem. Soc.* **2003**, *125*, 13976–13977. (d) Pardo, E.; Ruiz-García, R.; Lloret, F.; Faus, J.; Julve, M.; Journaux, Y.; Delgado, F.; Ruiz- Pe′rez, C. *Adv. Mater.* **2004**, *16*, 1597–1600. (e) Kajiwara, T.; Nakano, M.; Kaneko, Y.; Takaishi, S.; Ito, T.; Yamashita, M.; Igashira-Kamiyama, A.; Nojiri, H.; Ono, Y.; Kojima, N. *J. Am. Chem. Soc.* **2005**, *127*, 10150–10151.

10.1021/ic702473y CCC: $40.75

materials is to organize paramagnetic centers into polynuclear or polymeric aggregates by the use of bridging ligands.[16] It is well-known that a carboxylate group can act as a bridging ligand, which leads to various polynuclear complexes ranging from discrete molecules to 3D networks.[17–19] Some short bridging ligands such as cyanide,[20,21] dicyanamide,[22] oxalate,[23] and azide(N_3^-)[24–26] have also been used to bridge metal ions to construct molecule-based magnetic materials. To search for new multifunctional coordination polymers with interesting magnetic properties, Htmopa was our ligand of choice. In comparison with the benzene-based,[27–30] naphthalene-based and anthracene-based carboxylic acids,[31–33] single crystals containing phenanthrene-based car-

---

(7) (a) Zheng, Y. Z.; Tong, M. L.; Xue, W.; Zhang, W. X.; Chen, X. M.; Grandjean, F.; Long, G. J. *Angew. Chem., Int. Ed.* **2007**, *46*, 6076–6080. (b) Manoli, M.; Johnstone, R. D. L.; Parsons, S.; Murrie, M.; Affronte, M.; Evangelisti, M.; Brechin, E. K. *Angew. Chem., Int. Ed.* **2007**, *46*, 4456–4460. (c) Gao, E. Q.; Yue, Y. F.; Bai, S. Q.; He, Z.; Yan, C. H. *J. Am. Chem. Soc.* **2004**, *126*, 1419–1429. (d) Chen, H. J.; Mao, Z. W.; Gao, S.; Chen, X. M. *Chem. Commun.* **2001**, 2320–2321. (e) Humphrey, S. M.; Wood, P. T. *J. Am. Chem. Soc.* **2004**, *126*, 13236–13237.

(8) (a) Li, M.; Xiang, J. F.; Yuan, L. J.; Wu, S. M.; Chen, S. P.; Sun, J. T. *Cryst. Growth Des.* **2006**, *6*, 2036–2040. (b) Pang, J.; Marcotte, E. J. P.; Seward, C.; Brown, R. S.; Wang, S. *Angew. Chem., Int. Ed.* **2001**, *40*, 4042–4045. (c) Zheng, S. L.; Yang, J. H.; Yu, X. L.; Chen, X. M.; Wong, W. T. *Inorg. Chem.* **2004**, *43*, 830–838. (d) He, J. H.; Yu, J. H.; Zhang, Y. T.; Pan, Q. H.; Xu, R. R. *Inorg. Chem.* **2005**, *44*, 9279–9282. (e) Zhang, X. M.; Tong, M. L.; Gong, M. L.; Chen, X. M. *Eur. J. Inorg. Chem.* **2003**, 138–142.

(9) (a) Bauer, C. A.; Timofeeva, T. V.; Settersten, T. B.; Patterson, B. D.; Liu, V. H.; Simmons, B. A.; Allendorf, M. D. *J. Am. Chem. Soc.* **2007**, *129*, 7136–7144. (b) Fang, Q. R.; Zhu, G. S.; Jin, Z.; Ji, Y. Y.; Ye, J. W.; Xue, M.; Yang, H.; Wang, Y.; Qiu, S. L. *Angew. Chem., Int. Ed.* **2007**, *46*, 6638–6642.

(10) (a) Cariati, E.; Macchi, R.; Roberto, D.; Ugo, R.; Galli, S.; Masciocchi, N.; Sironi, A. *Chem. Mater.* **2007**, *19*, 3704–3711. (b) Thalladi, V. R.; Brasselet, S.; Bläser, D.; Boese, R.; Zyss, J.; Nangia, A.; Desiraju, G. R. *Chem. Commun* **1997**, 1841–1842. (c) Lin, W. B.; Evans, O. R.; Xiong, R. G.; Wang, Z. Y. *J. Am. Chem. Soc.* **1998**, *120*, 13272–13273. (d) Cariati, E.; Macchi, R.; Roberto, D.; Ugo, R.; Galli, S.; Casati, N.; Macchi, P.; Sironi, A.; Bogani, L.; Caneschi, A.; Gatteschi, D. *J. Am. Chem. Soc.* **2007**, *129*, 9410–9420.

(11) Adams, R. D.; Cotton, F. A. *Catalysis by Di- and Polynuclear Metal Cluster Complexes*; Wiley-VCH: New York, 1998.

(12) (a) Kahn, O. *Molecular Magnetism*; VCH: New York, 1993. (b) Miller, J. S., Drilon, M., Eds; *Magnetism: Molecules to Materials*; Wiley-VCH: Weinheim, Germany, 2002.

(13) Gatteschi, D.; Sessoli, R. *Angew. Chem., Int. Ed.* **2003**, *42*, 268–297.

(14) Miyasaka, H.; Madanbashi, T.; Sugimoto, K.; Nakazawa, Y.; Wernsdorfer, W.; Sugiura, K. I.; Yamashita, M.; Coulon, C.; Clérac, R. *Chem.—Eur. J.* **2006**, *12*, 7028–7040.

(15) Caneschi, A.; Gatteschi, D.; Lalioti, N.; Sangregorio, C.; Sessoli, R.; Venturi, G.; Vindigni, A.; Rettori, A.; Pini, M. G.; Novak, M. A. *Angew. Chem., Int. Ed.* **2001**, *40*, 1760–1763.

(16) Gao, E. Q.; Cheng, A. L.; Xu, Y. X.; He, M. Y.; Yan, C. H. *Inorg. Chem.* **2005**, *44*, 8822–8835.

(17) Colacio, E.; Ghazi, M.; Kivekäs, R.; Moreno, J. M. *Inorg. Chem.* **2000**, *39*, 2882–2890.

(18) Rettig, S. J.; Thompson, R. C.; Trotter, J.; Xia, S. *Inorg. Chem.* **1999**, *38*, 1360–1363.

(19) Tangoulis, V.; Psomas, G.; Dendrinou-Samara, C.; Raptopoulou, C. P.; Terzis, A.; Kessissoglou, D. P. *Inorg. Chem.* **1996**, *35*, 7655–7660.

(20) (a) Prins, F.; Pasca, E.; de Jongh, L. J.; Kooijman, H.; Spek, A. L.; Tanase, S. *Angew. Chem., Int. Ed.* **2007**, *46*, 6081–6084. (b) Mallah, T.; Thiebaut, S.; Verdaguer, M.; Veillet, P. *Science* **1993**, *262*, 1554–1557. (c) Entley, W. R.; Girolami, G. S. *Science* **1995**, *268*, 397–400. (d) Verdaguer, M.; Bleuzen, A.; Marvaud, V.; Vaissermann, J.; Seuleiman, M.; Desplanches, C.; Scuiller, A.; Train, C.; Garde, R.; Gelly, G.; Lomenech, C.; Rosenman, I.; Veillet, P.; Cartier, C.; Villain, F. *Coord. Chem. Rev.* **1999**, *192*, 1023–1047. (e) Tanase, S.; Reedijk, J. *Coord. Chem. Rev.* **2006**, *250*, 2501–2510. (f) Ohba, M.; Okawa, H. *Coord. Chem. Rev.* **2000**, *198*, 313–328.

(21) (a) Herrera, J. M.; Marvaud, V.; Verdaguer, M.; Marrot, J.; Kalisz, M.; Mathoniere, C. *Angew. Chem., Int. Ed.* **2004**, *43*, 5468–5471. (b) Ohkoshi, S.; Tokoro, H.; Hozumi, T.; Zhang, Y.; Hashimoto, K.; Mathoniere, C.; Bord, I.; Rombaut, G.; Verelst, M.; Moulin, C. C. D.; Villain, F. *J. Am. Chem. Soc.* **2006**, *128*, 270–277. (c) Sieklucka, B.; Podgajny, R.; Przychodzen, P.; Korzeniak, T. *Coord. Chem. Rev.* **2005**, *249*, 2203–2221. (d) Zhang, Y. Z.; Wang, Z. M.; Gao, S. *Inorg. Chem.* **2006**, *45*, 5447–5454.

(22) Jensen, P.; Price, D. J.; Batten, S. R.; Moubaraki, B.; Murray, K. S. *Chem.—Eur J.* **2000**, *6*, 3186–3195.

(23) (a) Decurtins, S.; Pellaux, R.; Antorrena, G.; Palacio, F. *Coord. Chem. Rev.* **1999**, *192*, 841–854. (b) Pellaux, R.; Schmalle, H. W.; Huber, R.; Fischer, P.; Hauss, T.; Ouladdiaf, B.; Decurtins, S. *Inorg. Chem.* **1997**, *36*, 2301–2308. (c) Decurtins, S.; Schmalle, H. W.; Pellaux, R.; Schneuwly, P.; Hauser, A. *Inorg. Chem.* **1996**, *35*, 1451–1460.

(24) (a) Ge, C. H.; Cui, A. L.; Ni, Z. H.; Jiang, Y. B.; Zhang, L. F.; Ribas, J.; Kou, H. Z. *Inorg. Chem.* **2006**, *45*, 4883–4885. (b) Koner, S.; Saha, S.; Mallah, T.; Okamoto, K. I. *Inorg. Chem.* **2004**, *43*, 840–842. (c) Song, Y.; Massera, C.; Roubeau, O.; Gamez, P.; Lanfredi, A. M. M.; Reedijk, J. *Inorg. Chem.* **2004**, *43*, 6842–6847. (d) Liu, C. M.; Yu, Z.; Xiong, R. G.; Liu, K.; You, X. Z. *Inorg. Chem. Commun.* **1999**, *2*, 31–34.

(25) (a) Domínguez-Vera, J. M.; Suárez-Varela, J.; Maimoun, I. B.; Colacio, E. *Eur. J. Inorg. Chem.* **2005**, 1907–1912. (b) Murugesu, M.; Habrych, M.; Wernsdorfer, W.; Abboud, K. A.; Christou, G. *J. Am. Chem. Soc.* **2004**, *126*, 4766–4767. (c) Papaefstathiou, G. S.; Perlepes, S. P.; Escuer, A.; Vicente, R.; Font- Bardia, M.; Solans, X. *Angew. Chem., Int. Ed.* **2001**, *40*, 884–886.

(26) (a) Halcrow, M. A.; Sun, J. S.; Huffman, J. C.; Christou, G. *Inorg. Chem.* **1995**, *34*, 4167–4177. (b) Karmakar, T. K.; Chandra, S. K.; Ribas, J.; Mostafa, G.; Lu, T. H.; Ghosh, B. K. *Chem. Commun.* **2002**, 2364–2365. (c) Zhang, L.; Tang, L. F.; Wang, Z. H.; Du, M.; Julve, M.; Lloret, F.; Wang, J. T. *Inorg. Chem.* **2001**, *40*, 3619–3622. (d) Ma, D. Q.; Hikichi, S.; Akita, M.; Moro-oka, Y. *J. Chem. Soc., Dalton Trans.* **2000**, 1123–1134.

(27) (a) Zhang, X. M.; Tong, M. L.; Chen, X. M. *Angew. Chem., Int. Ed.* **2002**, *41*, 1029–1031. (b) Kirillov, M.; Kopylovich, M. N.; Kirillova, M. V.; Haukka, M.; Guedes da Silva, M. F. C.; Pombeiro, A. J. L. *Angew. Chem., Int. Ed.* **2005**, *44*, 4345–4349. (c) Du, M.; Jiang, X. J.; Zhao, X. J. *Chem. Commun.* **2005**, 5521–5523. (d) Li, X. H.; Yang, S. Z.; Xiao, H. P. *Cryst. Growth Des.* **2006**, *6*, 2392–2397. (e) Hu, T. L.; Li, J. R.; Liu, C. S.; Shi, X. S.; Zhou, J. N.; Bu, X. H.; Ribas, J. *Inorg. Chem.* **2006**, *45*, 162–173. (f) Company, A.; Gómez, L.; Valbuena, J. M. L.; Mas-Ballesté, R.; Benet-Buchholz, J.; Llobet, A.; Costas, M. *Inorg. Chem.* **2006**, *45*, 2501–2508.

(28) (a) Huang, Z. L.; Drillon, M.; Masciocchi, N.; Sironi, A.; Zhao, J. T.; Rabu, P.; Panissod, P. *Chem. Mater.* **2000**, *12*, 2805–2812. (b) Rosi, N. L.; Kim, J.; Eddaoudi, M.; Chen, B.; O′Keeffe, M.; Yaghi, O. M. *J. Am. Chem. Soc.* **2005**, *127*, 1504–1518.

(29) (a) Groeneman, R. H.; MacGillivray, L. R.; Atwood, J. L. *Inorg. Chem.* **1999**, *38*, 208–209. (b) Go, Y. B.; Wang, X.; Anokhina, E. V.; Jacobson, A. J. *Inorg. Chem.* **2004**, *43*, 5360–5367. (c) Go, Y. B.; Wang, X.; Anokhina, E. V.; Jacobson, A. J. *Inorg. Chem.* **2005**, *44*, 8265–8271. (d) Cano, J.; Munno, G. D.; Sanz, J. L.; Ruiz, R.; Faus, J.; Lloret, F.; Julve, M.; Caneschi, A. *J. Chem. Soc., Dalton Trans.* **1997**, 1915–1923. (e) Hong, C. S.; You, Y. S. *Polyhedron* **2004**, *23*, 1379–1384.

(30) (a) Gavrilenko, K. S.; Punin, S. V.; Cador, O.; Golhen, S.; Ouahab, L.; Pavlishchuk, V. V. *J. Am. Chem. Soc.* **2005**, *127*, 12246–12253. (b) Biradha, K.; Seward, C.; Zaworotko, M. J. *Angew. Chem., Int. Ed.* **1999**, *38*, 492.

(31) (a) Maji, T. K.; Ohba, M.; Kitagawa, S. *Inorg. Chem.* **2005**, *44*, 9225–9231. (b) Lu, J. Y.; Schauss, V. *Inorg. Chem. Commun.* **2002**, *5*, 1028–1030. (c) Maji, T. K.; Kaneko, W.; Ohba, M.; Kitagawa, S. *Chem. Commun.* **2005**, 4613–4615. (d) Zheng, X. J.; Li, L. C.; Gao, S.; Jin, L. P. *Polyhedron* **2004**, *23*, 1257–1262. (e) Chun, H.; Dybtsev, D. N.; Kim, H.; Kim, K. *Chem.—Eur. J.* **2005**, *11*, 3521–3529. (f) Shan, N.; Bond, A. D.; Jones, W. *Tetrahedron Lett.* **2002**, *43*, 3101–3104. (g) Bickley, J. F.; Bonar-Law, R. P.; Femoni, C.; MacLean, E. J.; Steiner, A.; Teat, S. J. *J. Chem. Soc., Dalton Trans.* **2000**, 4025–4027. (h) Bonar-Law, R. P.; McGrath, T. D.; Singh, N.; Bickley, J. F.; Steiner, A. *Chem. Commun.* **1999**, 2457–2458. (i) Yang, J.; Yue, Q.; Li, G. D.; Cao, J. J.; Li, G. H.; Chen, J. S. *Inorg. Chem.* **2006**, *45*, 2857–2865.

(32) (a) Liu, C. S.; Shi, X. S.; Li, J. R.; Wang, J. J.; Bu, X. H. *Cryst. Growth Des.* **2006**, *6*, 656–663. (b) Zou, R. Q.; Liu, C. S.; Shi, X. S.; Bu, X. H.; Ribas, J. *CrystEngComm* **2005**, *7*, 722–727. (c) Bu, X. H.; Tong, M. L.; Chang, H. C.; Kitagawa, S.; Batten, S. R. *Angew. Chem., Int. Ed.* **2004**, *43*, 192–195. (d) Bu, X. H.; Tong, M. L.; Xie, Y. B.; Li, J. R.; Chang, H. C.; Kitagawa, S.; Ribas, J. *Inorg. Chem.* **2005**, *44*, 9837–9846.

boxylic acid ligands had not previously been reported. The Htmopa ligand has three obvious characteristics: (1) it has a large conjugated π systems and therefore can combine with d^{10} metals to construct useful photoluminescence materials; (2) the $\pi \cdots \pi$ stacking and/or $C-H \cdots \pi$ interactions may play important roles in the formation of higher-dimensional supramolecular frameworks; (3) the steric hindrance of the bulky methoxy phenanthrene ring may not only affect the coordination abilities and ligating modes of carboxylic groups but also propagate magnetic superexchange between metal centers. In the present work, we have synthesized four new complexes with the Htmopa ligand, and their photoluminescent properties and magnetic properties have also been reported.

Experimental Section

Materials and Methods. All chemicals except Htmopa ligand were of reagent-grade quality from commercial sources and were used without further purification. The Htmopa ligand was prepared according to previous literature.[34] The IR absorption spectra of the complexes were recorded in the range of 400−4000 cm^{-1} by means of a Nicolet (Impact 410) spectrometer with KBr pellets (5 mg of sample in 500 mg of KBr). Carbon and hydrogen analyses were carried out with a PerkinElmer 240C elemental analyzer. Luminescent spectra were recorded with a SHIMAZU VF−320 X-ray fluorescence spectrophotometer at room temperature (25 °C). XRD measurements were performed on a Bruker D8 Advance X-ray diffractometer using Cu Kα radiation ($\lambda = 0.15418$ nm), in which the X-ray tube was operated at 40 kV and 40 mA. Temperature-dependent magnetic susceptibility data for polycrystalline **2**, **3**, and **4** were obtained on a SQUID XL-7 magnetometer under an applied field of 100 Oe over the temperature range of 1.8−300 K.

Caution. *Perchlorate complexes of metal ions are potentially explosive. Only a small amount of material should be prepared, and it should be handled with caution.*

Synthesis of $Zn_2(Htmopa)_4(H_2O)_4$ (1). $Zn(ClO_4)_2 \cdot 6H_2O$(74.47 mg, 0.2 mmol) was added to an aqueous solution of Htmopa (17 mg, 0.05 mmol), which was adjusted to pH ≈ 9.0 with triethylamine (Et_3N). The final mixture was sealed in a 15 mL PTFE-lined stainless-steel acid digestion bomb and heated at 150 °C for three days. The large quantities of white-block crystals were obtained, and crystals were filtered off, washed with copious quantities of distilled water, and dried under ambient conditions. Selected white-block crystals were detected by X-ray. The pure phase **1** was obtained by manual separation (yield: 60 mg, ca. 76% based on Htmopa). Anal. Calcd for $C_{76}H_{76}O_{28}Zn_2$: C, 58.21%, H 4.88%; found C, 58.18%, H, 4.89%. IR(KBr,cm^{-1}): 3482(s), 1618(m), 1550(w), 1508(s), 1472(s), 1426(s), 1252(vs), 1198(m), 1162(m), 1143(m), 1043(w), 993(w), 901(w), 780(w), 618 (w), 546(w).

Synthesis of $Mn_2(Htmopa)_4(H_2O)_4$ (2). **2** was prepared in the same way as that for **1** but using $MnCl_2 \cdot 2H_2O$ (24 mg, 0.15mmol) to replace $Zn(ClO_4)_2 \cdot 6H_2O$, the pH was adjusted to 9.0 with triethylamine (Et_3N), and yellow block crystals were obtained in a 53% yield based on Htmopa. Anal. Calcd for $C_{76}H_{76}O_{28}Mn_2$: C, 74.38%; H, 6.24%; Found: C, 74.40%; H, 6.22%. IR(KBr,cm^{-1}): 3468(vs), 1618(m), 1545(w), 1508(s), 1471(s), 1426(s), 1252(vs), 1197(m), 1143(m), 1041(w), 993(w), 899(w), 780(w), 665 (w), 550(w).

Synthesis of $\{Ni(Htmopa)_2(H_2O)_2\}_n$ (3). **3** was prepared in the same way as that for **1** but using $NiCl_2 \cdot 6H_2O$ (37 mg, 0.15mmol) to replace $Zn(ClO_4)_2 \cdot 6H_2O$, the pH was adjusted to 9.0 with dilute sodiumhydroxide (1 M/L), and green block crystals were obtained in a 70% yield based on Htmopa. Anal. Calcd for $C_{38}H_{38}O_{14}Ni$: C, 58.71%; H, 4.93%. Found: C, 58.68%; H, 4.85%. IR(KBr,cm^{-1}): 3604(w), 3506(m), 1616(m), 1570(m), 1508(s), 1471(s), 1429(s), 1253(vs), 1198(m), 1143(m), 1043(w), 1019(w), 891(w), 778(w), 670 (w), 549(w).

Synthesis of $\{Co(Htmopa)_2(H_2O)_2\}_n$ (4). **4** was prepared in the same way as that for **1** but using $CoCl_2 \cdot 6H_2O$(47.58 mg, 0.2mmol) to replace $Zn(ClO_4)_2 \cdot 6H_2O$, the pH was adjusted to 9.0 with triethylamine (Et_3N), and red block crystals were obtained in a 75% yield based on Htmopa. Anal. Calcd for $C_{38}H_{38}CoO_{14}$: C, 58.69%; H, 4.93%; Found: C, 58.75%; H, 4.91%. IR(KBr,cm^{-1}): 3610(w), 3502(m), 1616(m), 1568(m), 1508(s), 1471(s), 1428(s), 1252(vs), 1197(m), 1143(m), 1042(w), 1019(w), 892(w), 778(w), 669 (w), 548(w).

X-ray Crystallography. Single crystals of **1**−**4** were prepared by the methods described in the synthetic procedure. X-ray crystallographic data of **1**−**4** were collected at room temperature using epoxy-coated crystals mounted on glass fiber. All measurements were made on a Bruker Apex Smart CCD diffractometer with graphite-monochromated Mo Kα radiation ($\lambda = 0.71073$ Å). The structures were solved by direct methods, and the non-hydrogen atoms were located from the trial structure and then refined anisotropically with *SHELXTL* using full-matrix least-squares procedures based on F^2 values.[35] The hydrogen atom positions were fixed geometrically at calculated distances and allowed to ride on the parent atoms. The final difference Fourier maps were found to be featureless. The relevant crystallographic data are presented in Table 1, whereas the selected bond lengths and angles are given in Table S1 in the Supporting Information (CCDC 668431−668434).

Results and Discussion

Synthesis. Hydrothermal combination of divalent zinc or manganese and Htmopa ligand with addition of base afforded dimeric complexes $M_2(Htmopa)_4(H_2O)_4$ ($M = Zn^{2+}$ (**1**), Mn^{2+} (**2**)) in high yield. However, the combination of a divalent cobalt or nickel with the same ligand at the same pH condition afforded 1D chain structure complexes $\{M(Htmopa)_2(H_2O)_2\}_n$ ($M = Ni^{2+}$ (**3**), Co^{2+} (**4**)). Though crystals of **1** were obtained by the reaction of Htmopa and $Zn(ClO_4)_2 \cdot 6H_2O$, we also obtained **1** by using $ZnCl_2 \cdot 6H_2O$ to replace $Zn(ClO_4)_2 \cdot 6H_2O$ under the same reaction conditions. We tried to use N_3^- to substitute coordinated water molecules by the addition of NaN_3 during the synthesis process, but no complex consisting of N_3^- was obtained. It confirms that metal ions (zinc, manganese, nickel, and cobalt) have a tendency to coordinate with water molecules rather than N_3^- in the presence of Htmopa ligand. It should also be pointed out that these complexes were highly reproducible for repeated synthesis under the reaction conditions employed in this work.

---

(33) (a) Liu, C. S.; Wang, J. J.; Yan, L. F.; Chang, Z.; Bu, X. H.; Sañudo, E. C.; Ribas, J. *Inorg. Chem.* **2007**, *46*, 6299–6310. (b) Ma, S. Q.; Wang, X. S.; Collier, C. D.; Manis, E. S.; Zhou, H. C. *Inorg. Chem.* **2007**, *46*, 8499–8501.

(34) Buckley, T. F., III.; Rapoport, H. *J. Org. Chem.* **1983**, *48*, 4222–4232.

(35) *Brukek 2000, SMART (Version 5.0), SAINT-plus (Version 6), SHELXTL (Version 6.1), and SADABS (Version 2.03)*; Bruker AXS Inc.; Madison, WI.

Table 1. Crystallographic Data and Structure Refinement Details for Complexes

complex	**1**	**2**	**3**	**4**
formula	$C_{76}H_{76}O_{28}Zn_2$	$C_{76}H_{76}Mn_2O_{28}$	$C_{38}H_{38}NiO_{14}$	$C_{38}H_{38}CoO_{14}$
fw	1568	1547.25	777.39	777.61
cryst syst	triclinic	triclinic	triclinic	triclinic
space group	$P\bar{1}$	$P\bar{1}$	$P\bar{1}$	$P\bar{1}$
a (Å)	7.3330(16)	7.4383(12)	7.3523(15)	7.4524(12)
b (Å)	13.230(3)	13.330(2)	13.565(3)	13.623(2)
c (Å)	19.042(4)	19.116(3)	18.490(4)	18.469(3)
α (deg)	104.875(4)	104.740(3)	104.140(4)	104.144(3)
β (deg)	92.475(4)	91.435(4)	90.958(4)	90.345(3)
γ (deg)	104.551(4)	105.584(3)	103.544(4)	104.269(3)
V (Å^3)	1716.7(7)	1756.7(5)	1733.1(6)	1757.8(5)
Z	1	1	2	2
D_c (g cm^{-3})	1.517	1.463	1.490	1.469
μ (Mo Ka) (mm^{-1})	0.789	0.448	0.633	0.560
F(000)	816	806	812	810
cryst size (mm)	0.10 × 0.20 × 0.25	0.15 × 0.20 × 0.25	0.15 × 0.20 × 0.25	0.15 × 0.20 × 0.25
temperature (K)	293	293	293	293
θ min, max (deg)	1.72, 25.00	1.72, 25.00	2.19, 25.00	1.71, 25.00
total, unique data	8649, 5947	8817, 6071	8654, 5985	8824, 6078
R(int)	0.041	0.063	0.046	0.038
observed data [$I > 2\ \sigma(I)$]	4490	4191	4574	3883
Nref, Npar	5947, 494	6071, 478	5985, 481	6078, 489
R, wR2	0.0487, 0.0868,	0.0544, 0.0912	0.0494, 0.1216	0.0556, 0.0785
S	1.00	1.00	1.00	0.937
max. and av. shift/error	0.00, 0.00	0.00, 0.00	0.00, 0.00	0.000, 0.000
min. and max. resd dens (e·Å^{-3})	−0.414, 0.482	−0.340, 0.500	−0.539, 0.493	−0.572, 0.547

Structures of 1 and 2. Single-crystal X-ray diffraction analyses reveal that both complexes are isostructural and crystallize in the triclinic $P\bar{1}$ space group. Only structure **1** is described here in detail. The molecular structure of **1** contains the centrosymmetric binuclear $Zn_2(Htmopa)_4(H_2O)_4$ unit. The coordination geometries of Zn1 and Zn1A are shown in part a of Figure 1. Each zinc(II) atom is five-coordinated by three carboxylate oxygen atoms occupying the equatorial sites and two water oxygen atoms occupying the axial positions, with $Zn-O_{eq}$ and $Zn-O_{ax}$ distances of 1.952(2)−1.976(2) and 2.103(2)−2.119(3) Å, respectively. The angles of O7−Zn1−O8A, O2−Zn1−O7, and O2−Zn1−O8A are 135.35(9), 119.11(9), and 105.54(9), respectively, and the coordination geometry at zinc can be looked at as a distorted trigonal bipyramidal with an O14−Zn1−O13 angle of 172.43(10). Two central zinc atoms (Zn1, Zn1A) are bridged by four oxygen atoms from two Htmopa ligands and form a dimeric $Zn_2O_{10}C_2$ unit with Zn···Zn distances of 3.615 Å. The Htmopa ligand adopts two kinds of coordination fashions; one acts as monodentate ligand combined with one zinc atom and the other coordinated to two zinc atoms by its two carboxylate oxygen atoms as a bridge, acting as a bidentate bridging ligand.

The dimeric $Zn_2O_{10}C_2$ unit is assembled into a 1D chain through three types of intermolecular hydrogen bonds, O13−H13B···O1#1, O13−H13C···O1, and O13−H13C···O8#2 with the distances [d(D···A)] being 2.812(4), 2.907(4), and 2.975(4) Å respectively (part b of Figure 1, Table S2 in the Supporting Information). Two types of weak hydrogen bonds, O14−H14A···O10#3 (green dotted lines) and O14−H14B···O9#3 (red dotted lines) with the distances [d(D···A)] being 2.824(3) and 3.052(3) Å, respectively, connected the parallel chains into 2D layered structure, as depicted in Figure S1 in the Supporting Information. The adjacent layers were connected by C−H···π (yellow dotted lines) interactions into a 3D network, as depicted in part c of Figure 1.

Structures of 3 and 4. Both complexes have a similar unit cell and the same space group of $P\bar{1}$. Taking **3** as an example, ORTEP plots of **3** are depicted in part a of Figure 2. There exist two kinds of nickel atoms: Ni(1) and Ni(2). The distance of Ni(1) and Ni(2) is 3.676Å. Both nickel atoms are six-coordinated and exhibit distorted octahedral geometry. However, their coordination environment is different, Ni(1) is coordinated by four water molecules (O7, O7B, O8, O8A) (O7, O7B acting as bridging atoms), and the other two sites are completed by bridging oxygen atoms (O9, O9A) from two bidentate Htmopa ligands. Ni(2) is coordinated by two bridging oxygen atoms (O10A, O10C) from two bidentate Htmopa ligands and two other bridging oxygen atoms (O1, O1B) from two monodentate Htmopa ligands, and the residual sites are occupied by two bridging water molecules (O7, O7B). In this complex, the ligand adopts two kinds of coordination modes: one acts as bidentate ligand to connect two nickle atoms by its two carboxylic oxygen atoms and forms a wavelike chain (part b of Figure 2, blue line); the other acts as a monodentate ligand. There also exist two kinds of coordinated water molecules: one acts as a bridging ligand to connect two nickle atoms and form a wavelike chain (part b of Figure 2, purple line). Another kind of water molecules acts as a terminal ligand. There are four types of intramolecular hydrogen bonds, O7−H7B···O8, O7−H7B···O9, O8−H8A···O1#1, and O8−H8B···O2, with the distances [d(D···A)] being 2.942(3), 2.796(3), 2.707(3), and 3.250(4) Å, respectively, between water and carboxylic oxygen atoms (Figure S2 and Table S2 in the Supporting Information) within the 1D chain. A 2D structure is assembled through intermolecular hydrogen bonds, O8−H8B···O13#2 with the

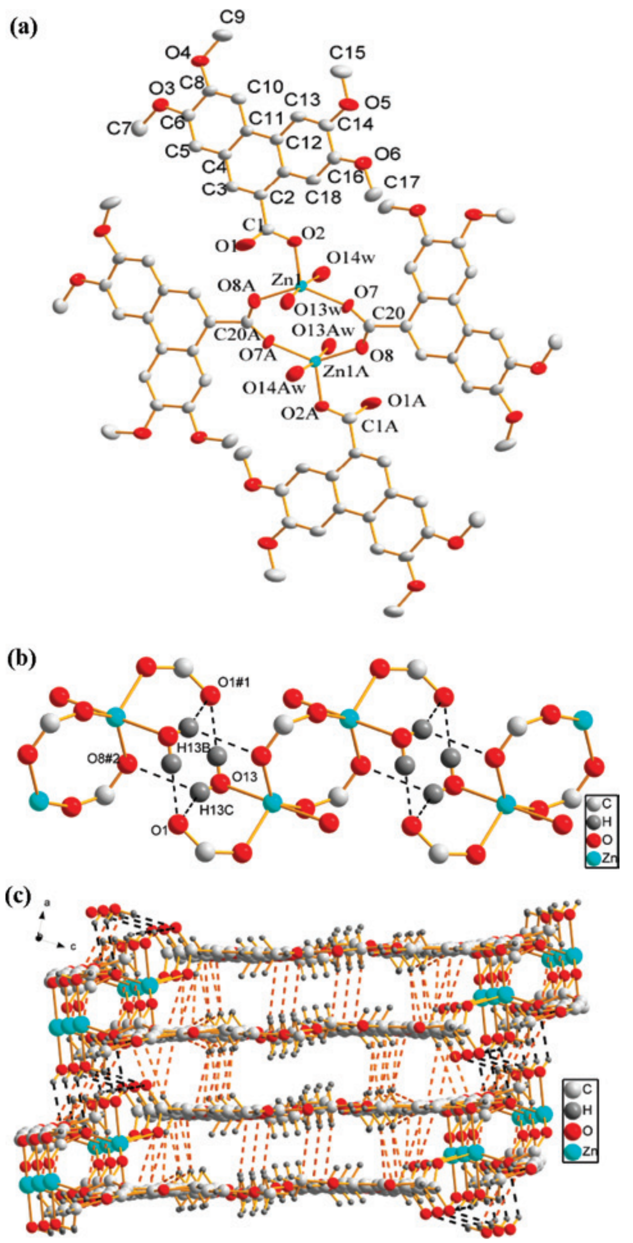

Figure 1. (a) An ORTEP drawing of **1** showing 50% ellipsoid probability (hydrogen atoms are omitted for clarity). Atoms labeled with the suffixes A is at the symmetry positions: $-x$, $-y$, $-z$. (b) View of 1D chain structure of **1** connected by hydrogen bonds depicted by the black dotted lines [symmetry code: #1 = $1 - x$, $-y$, $-z$; #2 = $1 + x$, y, z]. (c) 3D networks connected by hydrogen bonds (black dotted lines) and C−H···π (orange dotted lines) interactions of **1**.

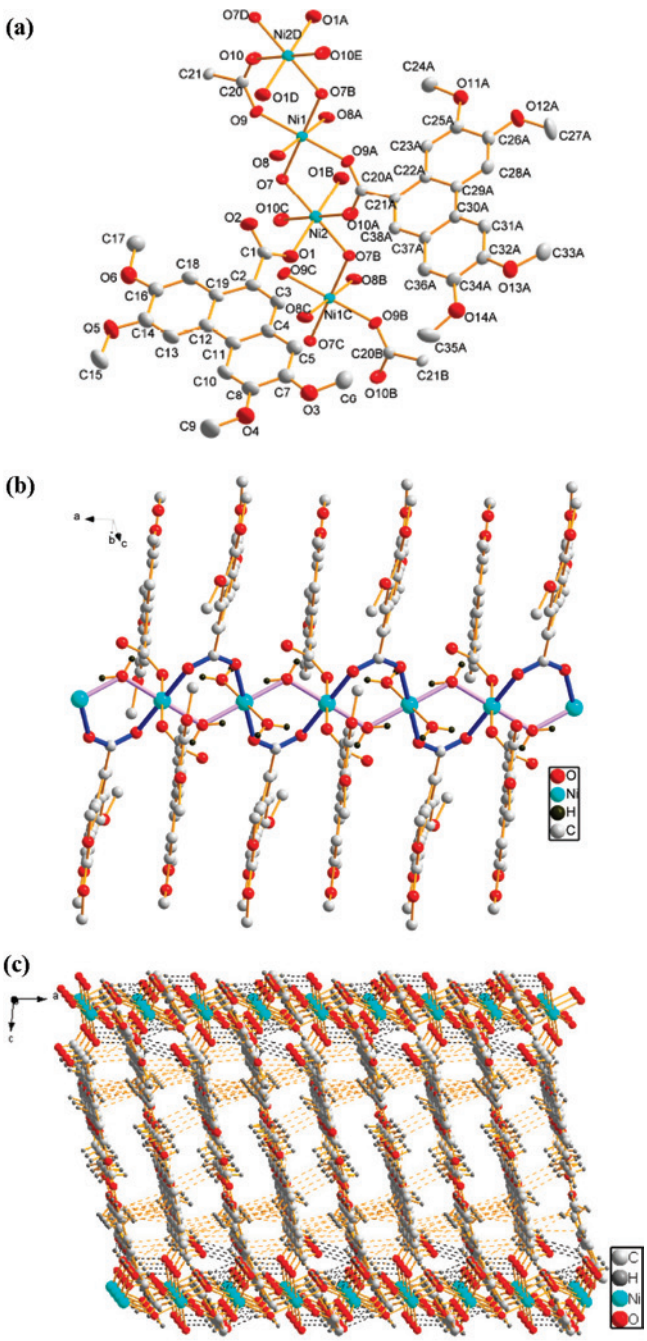

Figure 2. (a) An ORTEP drawing of **3** showing 50% ellipsoid probability (hydrogen atoms are omitted for clarity). Atoms labeled with the suffixes A, B, C, D, and E are at the symmetry positions (A) $1 - x$, $1 - y$, $1 - z$; (B) $-x$, $1 - y$, $1 - z$; (C) $-1 + x$, y, z; (D) $1 + x$, y, z; (E) $2 - x$,$1 - y$,$1 - z$. (b) Perspective view of the double-strand chain structure of **3** (hydrogen atoms of aromatic rings have been omitted for clarity). (c) 3D networks connected by hydrogen bonds (black dotted lines) and C−H···π (yellow dotted lines) interactions of complex **3**.

distance [d(D···A)] being 2.905(3) Å (Figure S3 and Table S2 in the Supporting Information). The adjacent layers were connected by C−H···π (yellow dotted lines) interactions into a 3D network, as depicted in part c of Figure 2.

Photoluminescence. During the past few years, the photoluminescent properties of many d^{10} metal coordination polymers have been studied, and the studies reveal that their luminescence behaviors are closely associated with the central metal ions and the ligands coordinated with them.[36–38] The photoluminescent properties of the free Htmopa ligand and **1**, **2**, **3**, and **4** have been investigated in the solid state at room temperature. The free Htmopa ligand displays strong luminescence with an emission maximum at 455 nm (λ_{ex} = 360 nm), which is can be assigned to the $\pi\cdots\pi^*$ transitions of the phenanthrene ring, and **1** exhibits a strong blue

---

(36) Li, M.; Xiang, J. F.; Yuan, L. J.; Wu, S. M.; Chen, S. P.; Sun, J. T. *Cryst. Growth Des.* **2006**, *6*, 2036–2040.

(37) (a) Zang, S. Q.; Su, Y.; Li, Y. Z.; Ni, Z. P.; Meng, Q. J. *Inorg. Chem.* **2006**, *45*, 2972–2978. (b) Mahata, P.; Natarajan, S. *Eur. J. Inorg. Chem.* **2005**, 2156–2163. (c) Zheng, S. L.; Yang, J. H.; Yu, X. L.; Chen, X. M.; Wong, W. T. *Inorg. Chem.* **2004**, *43*, 830–838. (d) Zheng, S. L.; Zhang, J. P.; Chen, X. M.; Huang, Z. L.; Lin, Z. Y.; Wong, W. T. *Chem.-Eur. J* **2003**, *9*, 3888–3896.

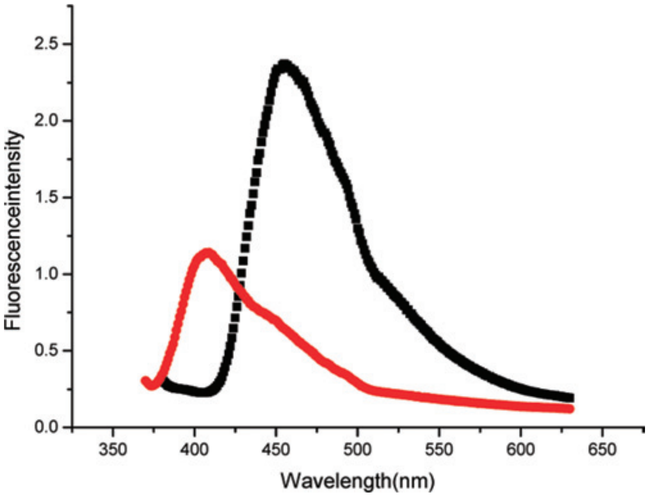

Figure 3. Emission spectra of free Htmopa ligand (black dotted lines) and **1** (red dotted lines) in the solid state at room temperature (λ_{ex} = 360 and 362 nm, respectively).

emission with λ_{max} = 409 nm upon excitation at 362 nm, and its luminescence can be assigned to ligand-to-metal charge transfer (LMCT).[8c,39,40] Compared with the fluorescent emission of ligand, the emission of **1** is blue-shifted and half-reduced (Figure 3) and emissions of **2**, **3**, and **4** are not observed in the solid state, which may be attributed to the effect of the central metal ion and coordinated water molecules.

Magnetic properties of 2, 3, and 4. The magnetic measurements were performed on polycrystalline samples of **2**, **3** and **4** using a SQUID magnetometer. The temperature dependence of magnetic susceptibility of **2** in the forms of χ_M and $\chi_M T$ versus T is displayed in Figure 4. As the temperature cools, $\chi_M T$ continuously decreases from 8.66 cm^3 K mol^{-1} at 300 K to 0.49 cm^3 K mol^{-1} at 1.8 K, indicating the antiferromagnetic coupling between manganese ions. From the viewpoint of crystal structure, **2** can be considered as an isolated spin dimer system, and the magnetic susceptibility in whole temperature range was fitted to eq 1, which is deduced from spin Hamiltonian $\hat{H} = -2J\vec{S}_1\vec{S}_2$,

$$\chi = \frac{2Ng^2\beta^2}{kT} \times \frac{e^{2J/kT} + 5e^{6J/kT} + 14e^{12J/kT} + 30e^{20J/kT} + 55e^{30J/kT}}{1 + 3e^{2J/kT} + 5e^{6J/kT} + 7e^{12J/kT} + 9e^{20J/kT} + 11e^{30J/kT}} \quad (1)$$

where all of the symbols have their normal meanings. The best fitting gave $J = -0.95(1)$ cm^{-1} with a reasonable g factor (2.023(1)) and $R = 5.6 \times 10^{-4}$ ($R = \sum[(\chi_M T)_{calcd} - (\chi_M T)_{obs}]^2/\sum(\chi_M T)^2_{obs}$). The calculated g factor is closed to the measurement result of 2.03 by EPR.

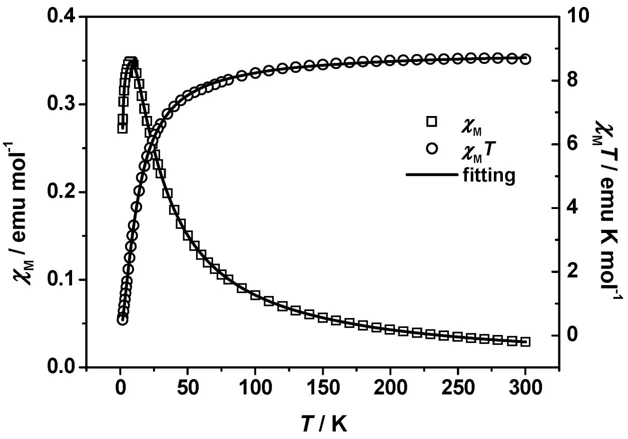

Figure 4. Temperature dependence of magnetic susceptibility in the form of χ_M and $\chi_M T$ vs T for **2**.

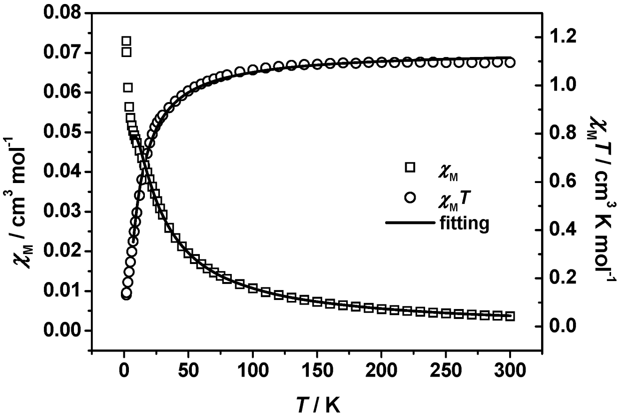

Figure 5. Temperature dependence of magnetic properties for **3**. The solid line is the fitting result from 7 to 300 K described in text.

For **3** as shown in Figure 5, the $\chi_M T$ products slowly decrease from 1.09 cm^3 K mol^{-1} at room temperature until 50 K, then quickly go down to 0.13 cm^3 K mol^{-1} at 1.8 K, indicating antiferromagnetic coupling between Ni^{II} ions in the system. The single-crystal structure suggests that **3** is a uniform 1D chain. So, the magnetic model in literature[41] can be used here for estimating the coupling interaction between Ni^{II} ions as follows:

$$\chi_M = (2Ng^2\beta^2/3kT)(\chi_r T_r) \quad (2)$$

$$\chi_r = [AT_r + BT_r + C]/[T_r + DT_r + ET_r + F] \quad (3)$$

where $T_r = kT/|J|$, J is the coupling constant between nickel ions and $A-F$ polynomial expressions of the alternate parameter can be obtained from $X(\alpha) = x_0 + x_1\alpha + x_2\alpha^2$ in the literature. When $0.5 \le \alpha \le 1$:

$A = 1$
$B = 0.5$
$C = 0.1$
$D = 1.136963 + 0.748419\alpha$
$E = 1.605652 - 1.462219\alpha + 1.668971\alpha^2$
$F = 0.4447955 + 1.162769\alpha$.

---

(38) (a) Wang, R. H.; Han, L.; Jiang, F. L.; Zhou, Y. F.; Yuan, D. Q.; Hong, M. C. *Cryst. Growth Des.* **2005**, *5*, 129–135. (b) He, J. H.; Yu, J. H.; Zhang, Y. T.; Pan, Q. H.; Xu, R. R. *Inorg. Chem.* **2005**, *44*, 9279–9282. (c) Tao, J.; Yin, X.; Wei, Z. B.; Huang, R. B.; Zheng, L. S. *Eur. J. Inorg. Chem.* **2004**, 125–133.

(39) Valeur, B. *Molecular Fluorescence: Principles and Applications*; Wiley-VCH: Weinheim, 2002.

(40) (a) Blasse, G.; Bleijenberg, K. C.; Powell, R. C. *Structure and Bonding 42: Luminescence and Energy Transfer*; Springer-Verlag: Berlin, 1980. (b) Crosby, G. A.; Highland, R. G.; Truesedell, K. A. *Chem. Rev.* **1985**, *64*, 41–52. (c) Kutal, C. *Coord. Chem. Rev.* **1990**, *99*, 213–252. (d) Blasse, G.; König, E.; Padhye, S. B.; Sonawane, P. B.; West, D. X. *Structure and Bonding, 76*, Complex Chemistry; Springer-Verlag, Berlin, 1991.

(41) Borrás-Almenar, J. J.; Coronado, E.; Curely, J.; Georges, R. *Inorg. Chem.* **1995**, *34*, 2699–2704.

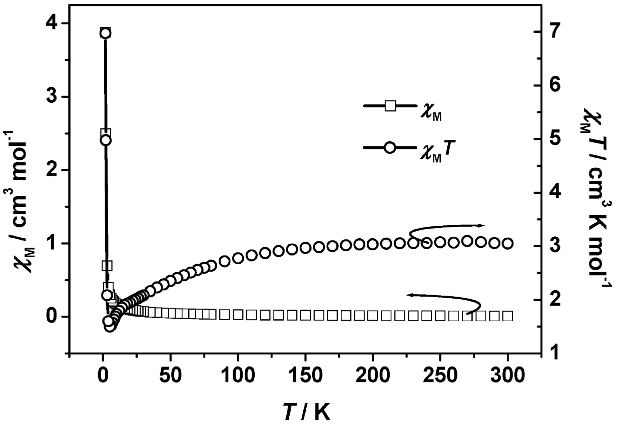

Figure 6. Temperature dependence of magnetic properties for **4**. Solid lines are the guide for eyes.

For the uniform chain, α = 1, the best fittings gave: $g = 2.14(1)$, $J = -4.13(4)$, and $R = 1.4 \times 10^{-4}$. This J value indicates the weak magnetic coupling exists between Ni^{II} ions within the chain in **3**.

3 and **4** are isostructural but the magnetic properties of **4** are very different from that of **3** because of the orbital contribution of Co^{II} ions as shown in Figure 6. At room temperature, $\chi_M T$ is equal to 3.05 cm^3·K·mol^{-1}, which is much higher than the spin-only value of 1.875 cm^3·K·mol^{-1} based on a Co^{II} ion ($g = 2$ and $s = {}^3/_2$) due to the spin–orbital coupling in **4**. Upon lowering the temperature, $\chi_M T$ continuously decreases and reaches a minimum of 1.50 cm^3·K·mol^{-1} at 5 K, and then abruptly increases to 7.0 cm^3·K·mol^{-1} at 1.8 K. In the higher temperature range above 5 K, the magnetic properties are dominated by single-ion behavior of the Co^{II} ion due to the depopulation of the excited levels ascribed to the splitting of $^4T_{2g}$ ground states under crystal field effects and spin–orbital coupling. Below 5 K, the increase of $\chi_M T$ obviously implies presence of ferromagnetic coupling between Co^{II} ions in **4**, and it is strong enough to compensate the decrease of $\chi_M T$ resulting from the effect of depopulation of the Kramer components of the Co^{II} ion. Thus, the dominant ferromagnetic properties were observed in the low-temperature range. In the temperature range of 300 to 30 K, the magnetic properties of **4** obey Curie–Weiss law (Figure S4 in the Supporting Information) and the fitting results gave $C = 3.29$ cm^3·K·mol^{-1} and $\theta = -18.7$ K, respectively. The negative Weiss constant indicates the single-ion behavior of Co^{II} ion in higher-temperature range.[42]

XRD Results. To confirm whether the crystal structures are truly representative of the bulk materials, XRD experiments have been carried out for **1**–**4**. The XRD experimental and computer-simulated patterns of the corresponding complexes are shown in Figure S5–S8 in the Supporting Information, which show that the bulk synthesized materials and the measured single crystals are homogeneous for **1**–**4**.

Conclusion

This contribution has described the synthesis and properties of the first phenanthrene-based carboxylic acid complexes, prepared by the hydrothermal reaction of transition metals with 2,3,6,7-tetramethoxyphenanthrene-9-carboxylic acid (Htmopa). We have success with introducing the bulky methoxy phenanthrene ligand into coordination polymers. **1** exhibits strong blue emissions. Magnetic susceptibility measurements indicate that **2** and **3** exhibit antiferromagnetic coupling, whereas **4** shows a ferromagnetic coupling and exhibits a single-ion behavior of the Co^{II} ion in higher temperature range. Possible applications of these materials can be foreseen as optical sensors or magnetic materials by virtue of their thermochromic and magnetic properties.

Acknowledgment. This work was supported by grants from the Natural Science Foundation of China (grants 20571039 and 20721002) and the National Basic Research Program of China (grant 2007CB925103).

Supporting Information Available: Crystallographic data in CIF format, selected bond distances and angles, hydrogen Bonding Geometry, additional figures, and XRD patterns of **1**, **2**, **3**, and **4**. This material is available free of charge via the Internet at http://pubs.acs.org.

IC702473Y

---

(42) Mabbs, F. E.; Machin, D. J. *Magnetism and Teansition Metal Complexes*; Chapman and Hall: London, 1973.